Letters

Series-Connected Current-Source Inverters: $f_{SW} = 60$ Hz

Ling Xing and Qiang Wei

***Abstract*—Pulsewidth-modulated series-connected current-source inverters (SC-CSIs) are a good candidate for high-voltage applications. In this letter, a new SC-CSI with a switching frequency of 60 Hz is proposed. Compared with the conventional one, the proposed inverter features lower switching losses, higher dc current utilization, and reduced passive component sizing.**

***Index Terms*—Current-source inverter, modulation scheme.**

I. Introduction

PULSEWIDTH-MODULATED (PWM) current-source inverters (CSIs) with a simple structure, a controllable power factor, and reliable short-circuit protection are well used in medium-voltage (MV) drives [1]–[6] and are attracting increased attention in microgrids [7]–[9], energy storage systems [10], and renewable energies [11], [12]. On this basis, series-connected CSIs (SC-CSIs) are formed by connecting a few such CSIs in series and are considered promising inverters for high-voltage applications [13]–[15].

The conventional SC-CSI is shown in Fig. 1, where identical CSIs are connected in series at input and in parallel at output through a multiwinding transformer and then to a common load, which can be either a grid network or other types of load. Considering the focus of this letter, an *RL* load is taken as an example. Here, the multiwinding transformer is an indispensable component, which provides a separate current path for each CSI to enable the operation of SC-CSIs. In addition, it is to match the voltages before and after if needed. All employed CSIs are identical in terms of topology, modulation, and control. The switching frequency of employed switches could be ranging from a couple of hundreds hertz to a few kilohertz depending on the power ratings of each CSI, as well as the used switches. For example, in high-power (megawatt-level) MV drives, the switching frequency of the switch is around 500 Hz [1]. To decrease switching losses and increase dc current utilization, a new type of SC-CSI with a switching frequency of 60 Hz is proposed. Compared with conventional SC-CSIs, the proposed one sees lower switching losses, higher dc current utilization, and reduced passive components. The following section presents the proposed SC-CSI in detail.

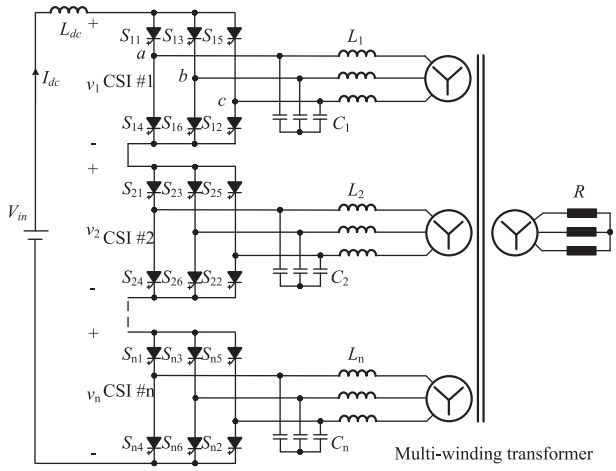

Fig. 1. Conventional SC-CSIs [13]–[15].

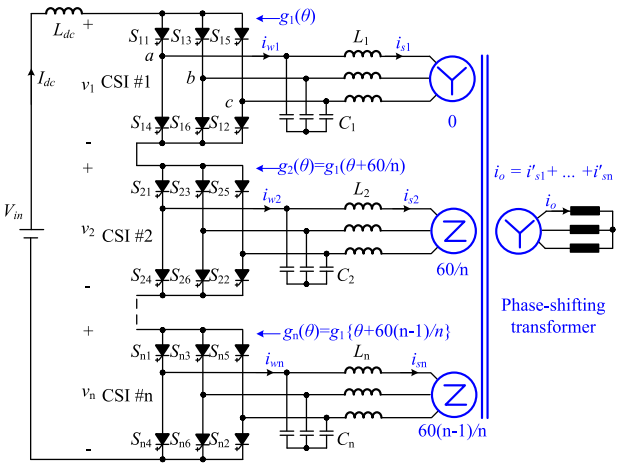

Fig. 2. Proposed SC-CSIs with $f_{sw} = 60$ Hz.

II. Proposed CSI: $f_{sw} = 60$ Hz

The proposed SC-CSI is shown in Fig. 2, in which three changes are made compared with the conventional one: 1) the switching frequency is reduced to 60 Hz; 2) a phase-shifting modulation is applied to CSI #*n*; and 3) a phase-shifting transformer is used, where the first is for switching loss reduction and

Manuscript received December 16, 2019; revised January 10, 2020 and February 5, 2020; accepted February 9, 2020. Date of publication February 18, 2020; date of current version May 1, 2020. *(Corresponding author: Qiang Wei.)*

Ling Xing is with the Thunder Bay, ON P7B 6A8, Canada (e-mail: kaierxing2006@126.com).

Qiang Wei is with the Department of Electrical Engineering, Lakehead University, Thunder Bay, ON P7B 5E1, Canada (e-mail: qwei@lakeheadu.ca).

Color versions of one or more of the figures in this article are available online at http://ieeexplore.ieee.org.

Digital Object Identifier 10.1109/TPEL.2020.2974734

TABLE I
PROPOSED MODULATION

Gating signals for *CSI* #1, $g_1(\theta)$							
θ	S_{11}	S_{12}	S_{13}	S_{14}	S_{15}	S_{16}	v_1
0-60°	1	0	0	0	0	1	v_{ab}
60°-120°	1	1	0	0	0	0	v_{ac}
120°-180°	0	1	1	0	0	0	v_{bc}
180°-240°	0	0	1	1	0	0	v_{ba}
240°-300°	0	0	0	1	1	0	v_{ca}
300°-360°	0	0	0	0	1	1	v_{cb}
Gating signals for *CSI* #n, $g_n(\theta) = g_1\{\theta + 60(n-1)/n\}$							
Phase shift of transformer for CSI #n, $60(n-1)/n$							

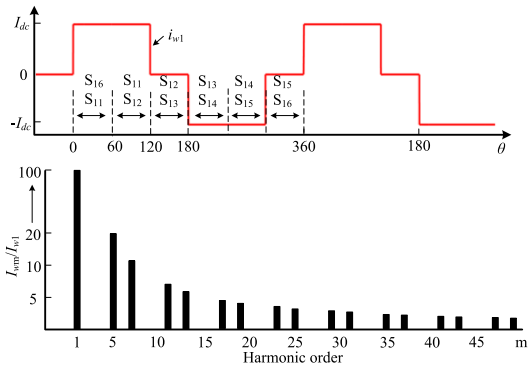

Fig. 3. Waveform of i_{w1} and its harmonics spectrum.

dc utilization maximization, while the last two are for harmonic elimination and passive component reduction.

A. 60-Hz Operation (Square-Wave Operation)

All switches are switching with a frequency of 60 Hz. Note that though there are a couple of modulations enabling a fundamental switching frequency [16], here, the simple one, i.e., square-wave operation, is taken as an example. Table I shows details of the switching scheme, and following this, the output PWM current, i_{w1}, as an example and its harmonics spectrum are illustrated in Fig. 3. Three well-proven conclusions are as follows: 1) very low switching losses due to $f_{\rm sw} = 60$ Hz; 2) the highest dc utilization at 0.78; and 3) significant low-order harmonics.

B. Phase-Shifting Modulation and Phase-Shifting Transformer

These significant low-order harmonics must be filtered out to meet requirements, such as IEEE 519. In conventional SC-CSIs, where the switching frequency is around 500 Hz or higher, there are no such substantial low-order harmonics, and the *LC* filter is used solely for harmonic elimination [1], [13]–[15]. However, here, in the proposed one, it is not favorable due to the requirements for very bulky and costly filters. On the other hand, a method of combining phase-shifting modulation and phase-shifting transformer is proposed to eliminate harmonics. In addition, passive components are reduced, thanks to the proposed scheme, which will be detailed in the following.

According to the operation principle of harmonic elimination of phase-shifting transformers, to enable harmonic elimination in the proposed SC-CSI, a phase-shifting angle (δ) among i_{wn} $(n = 1, 2, \ldots)$ is required, and this angle should be the same as that of the corresponding winding of the transformer. Following this, the required phase-shifting modulation is generated and shown in Table I. And by doing so, specific harmonics can be eliminated.

For example, for a two-CSI system, the phase shift is $\delta = 30^{\rm o}$, and the currents i_{s1} and i_{s2} (before the transformer) are

$$\begin{aligned} i_{s1} &= \sum_{m=1,3,5\ldots} I_m \sin(m\omega t) \\ i_{s2} &= \sum_{m=1,3,5\ldots} I_m \sin\{m(\omega t + 30^\circ)\}. \end{aligned} \tag{1}$$

The relationship between currents before and after the phase-shifting transformer in terms of the phase angle is [1]

$$\begin{aligned} \angle i'_{sn-m} &= \angle i_{sn-m} - \delta \quad \text{for positive-sequence harmonics} \\ \angle i'_{sn-m} &= \angle i_{sn-m} + \delta \quad \text{for negative-sequence harmonics} \end{aligned} \tag{2}$$

where i'_{sn-m} and i_{sn-m} refer to the *m*th-order harmonic currents of the currents i'_{sn} and i_{sn}, respectively.

Assuming the transformer with a voltage ratio of 1, the resultant load current i_o can be obtained by using (1) and (2), as follows:

$$\begin{aligned} i_o &= i'_{s1} + i'_{s2} \\ &= 2I_1 \sin(\omega t) + 2I_{11}\sin(11\omega t) + 2I_{13}\sin(13\omega t) + \cdots \end{aligned} \tag{3}$$

where the harmonic currents of 5th, 7th, 17th, 19th orders, etc., are eliminated. With more CSIs connected in series and sharing one phase-shifting transformer, more harmonic currents are eliminated. And the derivation of load current harmonics for any other *n*-CSI is obtained in the same way and has been thoroughly reported in [17]; thus, it is not repeated here.

C. Passive Component Reduction for an n-CSI

LC filter reduction is achieved due to harmonic elimination of the phase-shifting transformer. The leakage inductance of the transformer with a sizing of around 0.08–0.1 p.u. functions as the filter inductor, while the sizing of the capacitor is dependent on the minimum harmonic to be mitigated to meet the harmonic requirement. In the conventional inverter, the capacitor is set to 0.5 p.u. [1], while in this letter, it is reduced, thanks to harmonic elimination. For example, a capacitor of 0.14 p.u. works for a five-CSI. Refer to [17] for details regarding capacitor minimization. Given any specific *n*-CSI, the harmonic elimination of the phase-shifting transformer will be known, and the reduction in the capacitor can be obtained using the method in [17].

A reduction in the dc inductor is also achieved due to the phase-shifting modulation. The dc inductor is calculated as follows:

$$\begin{aligned} L_{\rm dc} &= \frac{\left(V_{\rm in} - \sum_{m=1}^{n} v_m\right)\Delta t}{\Delta I_{\rm dc}} \\ \sum_{m=1}^{n} v_m &= v_1 + \underbrace{v_1\left(\theta + \frac{60}{n}\right)}_{v_2} + \cdots + \underbrace{v_1\left(\theta + \frac{60(n-1)}{n}\right)}_{v_n} \end{aligned} \tag{4}$$

TABLE II
SIMULATION AND EXPERIMENT PARAMETERS

	Simulation	Experiment
I_{dc}	200 A	5 A
n-CSI	5	2
f_{sw}	60 Hz	60 Hz
C_n	22 μF (0.14 pu)	100 μF (0.38 pu)
L_n	4.6 mH (0.1 pu)	5 mH (0.18 pu)
R	3.5 Ω (1 pu)	10 Ω (1 pu)

where v_n is the input voltage for CSI #n, $\Delta I_{\rm dc}$ is the current ripple, 12%, for example, and Δt is the dwell time. As shown in Table I, neglecting the voltage drop on the load-side inductor, v_1 can be obtained by the load voltage, which is defined as follows:

$$\begin{cases} v_{\rm ab} = \sqrt{3}V_g\cos(\theta+\pi/6) \\ \vdots \\ v_{\rm ac} = \sqrt{3}V_g\cos(\theta-\pi/6) \end{cases} \tag{5}$$

where V_g is the load line-to-neutral voltage and θ is the phase angle [18].

Given any specific n-CSI, all variables involved in (4) and (5) will be known, and therefore, the dc inductor and its reduction in comparison with the conventional one can be obtained by solving (4) and (5). For example, $L_{\rm dc} = 48$ mH (2.1 p.u.) for a two-CSI system and $L_{\rm dc} = 8$ mH (0.88 p.u.) for a five-CSI system, while they are increased to 55 mH (2.4 p.u.) and $L_{\rm dc} =$ 137.5 mH (15 p.u.) with the conventional inverter [1], [14]. In both calculations, a single CSI is rated with 1 MVA/4160 V, and a dc current ripple of 12% is selected.

D. Discussion

First, phase-shifting transformer technology and manufacturing is mature [1]. Compared with the conventional one, the phase-shifting transformer has same voltage/current/power ratings and insulation level, but with a relatively complex winding connection, which, however, does not cause significant cost, if any, as the determining pricing factors are power rating and insulation level. Second, the proposed modulation scheme does not have the capability of $I_{\rm dc}$ control, and it is achieved by the control of the front-end rectifier [1].

III. PERFORMANCE INVESTIGATION

Simulation and laboratory-scaled experiments are conducted to demonstrate the performance of the proposed SC-CSI. The parameters used are listed in Table II.

A. Simulated Investigation

Fig. 4 shows the simulated waveforms of a five-CSI. The output PWM currents i_{w1}–i_{w5} are identical but with a phase shift of 12° between any two adjacent currents. Though the currents before (i_{s1}–i_{s5}) and after (i'_{s5}) the phase-shifting transformer are highly distorted due to significant low-order harmonics, the load current i_o performs excellent harmonic performance due to the harmonic elimination. The load current spectrum is shown in Fig. 5.

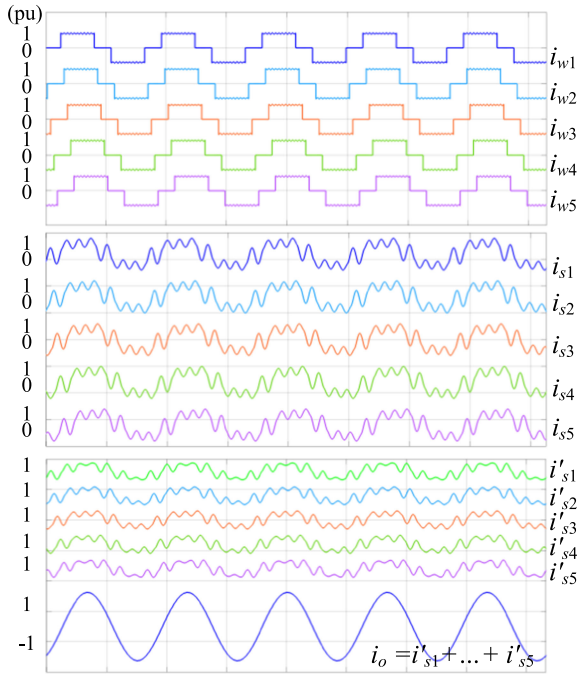

Fig. 4. Simulated waveforms for a five-CSI with the proposed scheme.

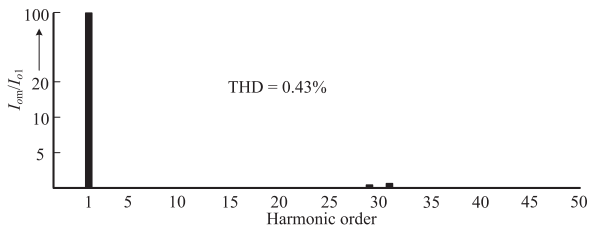

Fig. 5. Harmonics spectrum of load current i_o with the proposed scheme.

B. Experimental Investigation

A laboratory-scaled two-CSI setup is constructed to verify the proposed inverter. As shown in Fig. 6, the PWM output currents for CSI #1 (i_{w1}) and CSI #2 (i_{w2}) are with a phase shift of 30° and same as previous analysis, in which the currents before and after the phase-shifting transformer are highly distorted, while the load current i_o has good harmonic performance without increasing the filter.

However, in the experiments, the phase-shifting transformer with a phase shift of 30° is constructed by connecting three single-phase transformers in delta at the one side and wye on the other side. The turn ratio of each single-phase transformer is 1:1. Therefore, the current after the transformer, i'_{s2}, is reduced to $i_{s2}/\sqrt{3}$, as shown in Fig. 6. As a result, the fifth and seventh harmonics cannot be eliminated completely, as shown in Fig. 6. To verify this, a simulation with same parameters of the experiments is provided in Figs. 7 and 8.

As shown above, the proposed inverter operates under $f_{\rm sw} = 60$ Hz, which decreases switching losses and increases dc current utilization. In addition, a sizing reduction is obtained for passive components.

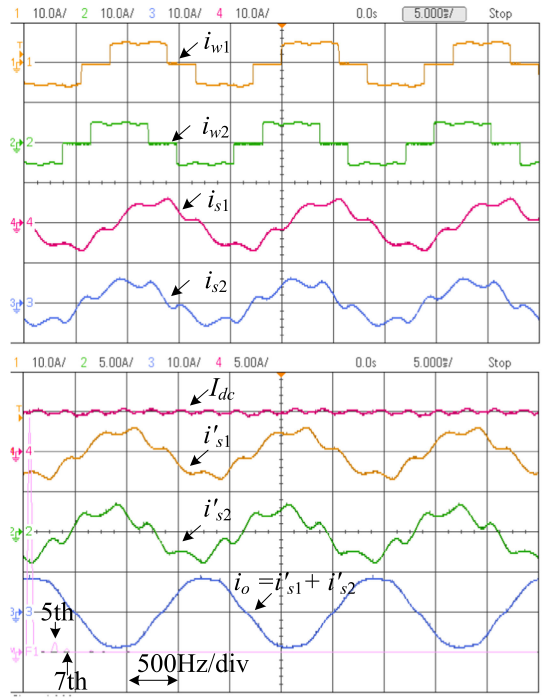

Fig. 6. Experimental waveforms of a five-CSI.

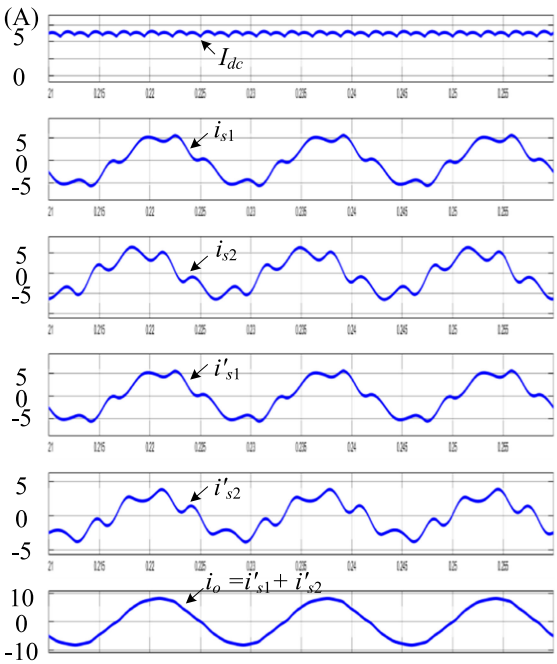

Fig. 7. Simulated waveforms with same parameters of experiments.

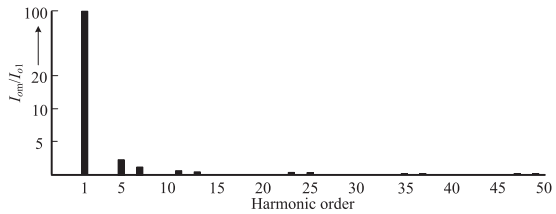

Fig. 8. Harmonics spectrum of i_o with same parameters of experiments.

IV. Conclusion

In this letter, a new SC-CSI is proposed. By combining phase-shifting modulation and the phase-shifting transformer, SC-CSIs operate with $f_{\rm sw} = 60$ Hz, contributing to both switching loss reduction and dc current utilization. Passive components are also reduced, thanks to the proposed scheme. A detailed design method for passive components is provided.

References

[1] B. Wu, *High-Power Converters and AC Drives*. Hoboken, NJ, USA: Wiley/IEEE Press, 2006.

[2] Y. W. Li, M. Pande, N. Zargari, and B. Wu, "Dc-link current minimization for high-power current-source motor drives," *IEEE Trans. Power Electron.*, vol. 24, no. 1, pp. 232–240, Jan. 2009.

[3] Y. W. Li, M. Pande, N. Zargari, and B. Wu, "Power factor compensation for PWM CSR-CSI fed high power drive system using flux adjustment," *IEEE Trans. Power Electron.*, vol. 24, no. 12, pp. 3014–3019, Dec. 2009.

[4] Z. Wang, B. Wu, D. Xu, and N. R. Zargari, "Hybrid pwm for high-power current-source-inverter-fed drives with low switching frequency," *IEEE Trans. Power Electron.*, vol. 26, no. 6, pp. 1754–1764, Jun. 2011.

[5] J. He, Q. Li, H. Wang, Y. Lyu, H. Jia, and C. Wang, "SVM strategies for simultaneous common-mode voltage reduction and dc current balancing in parallel current source converters," *IEEE Trans. Power Electron.*, vol. 33, no. 10, pp. 8859–8871, Oct. 2018.

[6] Z. Bai, Z. Zhang, and X. Ruan, "A natural soft-commutation PWM scheme for current source converter and its logic implementation," *IEEE Trans. Ind. Electron.*, vol. 58, no. 7, pp. 2772–2779, Jul. 2011.

[7] X. Guo, D. Xu, J. M. Guerrero, and B. Wu, "Space vector modulation for dc-link current ripple reduction in back-to-back current-source converters for microgrid applications," *IEEE Trans. Ind. Electron.*, vol. 62, no. 10, pp. 6008–6013, Oct. 2015.

[8] X. Guo, Y. Yang, and X. Wang, "Advanced control of grid-connected current source converter under unbalanced grid voltage conditions," *IEEE Trans. Ind. Electron.*, vol. 65, no. 12, pp. 9225–9233, Dec. 2018.

[9] J. He *et al.*, "A fault-tolerant operation approach for grid-tied five-phase current-source converters with one-phase supplying wire broken," *IEEE Trans. Power Electron.*, vol. 34, no. 7, pp. 6200–6218, Jul. 2019.

[10] Z. Wang, B. Yuwen, Y. Lang, and M. Cheng, "Improvement of operating performance for the wind farm with a novel CSC-type wind turbine-SMES hybrid system," *IEEE Trans. Power Del.*, vol. 28, no. 2, pp. 693–703, Apr. 2013.

[11] J. Dai, D. Xu, and B. Wu, "A novel control scheme for current-source converter-based PMSG wind energy conversion systems," *IEEE Trans. Power Electron.*, vol. 24, no. 4, pp. 963–972, Apr. 2009.

[12] S. Anand, S. K. Gundlapalli, and B. G. Fernandes, "Transformer-less grid feeding current source inverter for solar photovoltaic system," *IEEE Trans. Ind. Electron.*, vol. 61, no. 10, pp. 5334–5344, Oct. 2014.

[13] M. Popat, B. Wu, F. Liu, and N. Zargari, "Coordinated control of cascaded current source converter based offshore wind farms," *IEEE Trans. Sustain. Energy*, vol. 3, no. 3, pp. 557–565, May 2012.

[14] Q. Wei, B. Wu, D. Xu, and N. Zargari, "A medium frequency transformer-based wind energy conversion system used for current source converter based offshore wind farm," *IEEE Trans. Power Electron.*, vol. 32, no. 1, pp. 248–259, Jan. 2017.

[15] Q. Wei, B. Wu, D. Xu, and N. R. Zargari, "A new configuration using PWM current source converters in low-voltage turbine-based wind energy conversion systems," *IEEE J. Emerg. Sel. Topics Power Electron.*, vol. 6, no. 2, pp. 919–929, Jun. 2018.

[16] G. S. Kulothungan, A. K. Rathore, J. Rodriguez, and D. Srinivasan, "Fundamental device switching frequency control of current-fed nine-level inverter for solar application," *IEEE Trans. Ind. Appl.*, to be published.

[17] Q. Wei, B. Wu, D. Xu, and N. R. Zargari, "Minimization of filter capacitor for medium-voltage current-source converters based on natural sampling SVM," *IEEE Trans. Power Electron.*, vol. 33, no. 1, pp. 473–481, Jan. 2018.

[18] Q. Wei, B. Wu, D. Xu, and N. R. Zargari, "Power balancing investigation of grid-side series-connected current source inverters in wind conversion systems," *IEEE Trans. Ind. Electron.*, vol. 64, no. 12, pp. 9451–9460, Dec. 2017.